Proposal for a Novel Two-Beam Accelerator

Ya. S. Derbenev, Y. Y. Lau, and R. M. Gilgenbach
Intense Energy Beam Interaction Laboratory, Department of Nuclear Engineering, University of Michigan, Ann Arbor, Michigan 48109-2104
(Received 1 November 1993; revised manuscript received 16 February 1994)

A new configuration is proposed wherein a low-current beam is accelerated to high energies (tens of amps, tens of MeV) by a driver beam of high current and low energy (a few kiloamps, < 1 MeV). The annular driver beam excites the TM_{020} cavity mode of an accelerating structure which transfers its rf power to the on-axis secondary beam. Systematic variation of the driver beam radius provides the secondary beam with phase focusing and adjustable acceleration gradient. A proof-of-principle experiment is suggested.

PACS numbers: 41.75.−i, 29.17.+w

Compact electron and ion accelerators in the 10 MeV range have a wide range of applications, such as treatment of bulk materials, activation analysis, and medical radiation sources. To achieve such an energy at moderate levels of current (tens of amps) requires considerable power, and a natural candidate for a driver is the pulse power system [1,2]. Intense annular electron beams (a few kiloamps, < 1 MeV) extracted from such a system have been modulated efficiently, and the current modulations exhibit a high degree of amplitude and phase stability [3]. These modulated beams have been used to generate ultrahigh power microwaves [4,5] and to accelerate electrons to high energies [6]. They will be used as the driver in the two-beam accelerator to be proposed in this paper.

Various two-beam accelerators have been studied in the past [6–10]. There are significant differences in the present configuration, shown schematically in Fig. 1. The driver beam is an annular beam of radius r_0, carrying an ac current I_d at frequency ω. It passes through an accelerator structure, consisting of N cylindrical pillbox cavities. Each cavity has a radius $b = 5.52c/\omega$ so that ω is also the resonant frequency of the TM_{020} mode of the pillbox cavity (Fig. 1). The secondary beam is an on-axis pencil beam, carrying an ac current I_s ($I_s \ll I_d$), also at frequency ω. Since the rf electric fields of the TM_{020} mode have opposite signs in the outer region and in the inner region, the mode retards the annular driver beam but accelerates the on-axis secondary beam. As we shall see, if the driver beam radius is modulated axially, phase focusing and tunability in the output energy of the secondary beam can be achieved. This is the crucial feature of the present device, not shared by the prior works [6–10].

Thus, without the use of rf plumbing, the present scheme provides the gradual conversion of the primary beam power to the secondary beam over many accelerating gaps. Since the current modulation on the primary beam has been shown to be insensitive to the variations in the diode voltage and diode current [3], the effectiveness in the acceleration of the secondary beam is likewise insensitive to such variations.

To calculate the excitation of the TM_{020} mode by the primary beam, and the resultant acceleration of the secondary beam by this mode, we assume that the intense space charge on the beam does not alter the rf characteristic of the cavities [4,11,12]. We also assume that the individual pillbox cavities are electromagnetically isolated from each other when the beams are absent [13,14]. Since the cavities are excited mainly by the rf current I_d carried by the primary beam, the TM_{020} mode so excited *always decelerates* the primary beam electrons on the average (by conservation of energy). This is true whether the beam radius r_0 is larger or smaller than a, where $a = 2.405c/\omega$ is the radius of the rf electric field null of the TM_{020} mode [Fig. 2(a)]. The value of the rf electric field at r_0 then gives the deceleration gradient. In terms of the relativistic mass factor (γ_d), the energy loss by this driver beam as it traverses the nth cavity is given by

$$\frac{d\gamma_d}{dn} = -\Lambda\delta^2 \tag{1}$$

in a continuum description. In Eq. (1),

$$\Lambda = 0.066(\omega L/c)Q(I_d/1\ \mathrm{kA}) \tag{2}$$

is the dimensionless parameter that measures the strength of the cavity excitation by the primary beam,

$$\delta = J_0(\omega r_0/c) \approx -1.249(r_0 - a)/a\,, \tag{3}$$

Q is the quality factor of the TM_{020} mode, L is the cavity length, and J_0 is the Bessel function of the first kind of

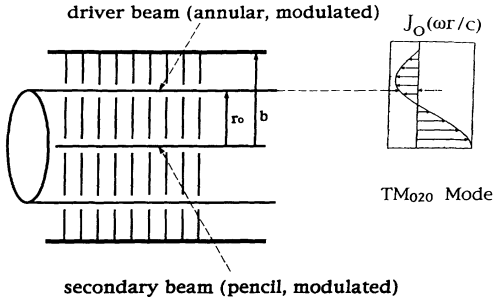

FIG. 1. Schematic drawing of the two-beam accelerator. Also shown is the rf force profile, $J_0(\omega r/c)$, associated with the axial electric field of the TM_{020} cavity mode.

0031-9007/94/72(19)/3025(4)$06.00

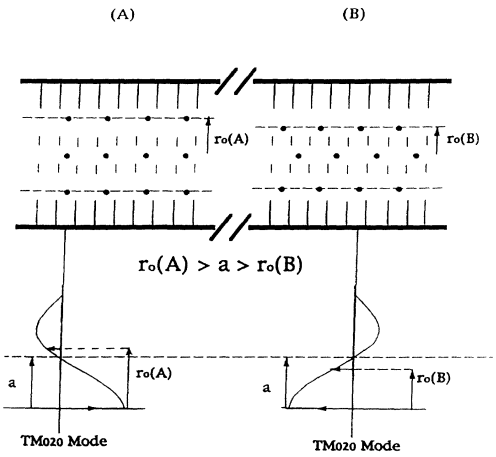

FIG. 2. (a) Position of the primary beam radius r_0 ($r_0 > a$) for secondary beam acceleration when both beams enter the cavity at the same phase. (b) Position of the primary beam radius r_0 ($r_0 < a$) for secondary beam acceleration when both beams enter the cavity at 180° phase apart.

order zero. In writing the last expression of Eq. (3), we have made the assumption that the annular beam is located in the vicinity of the rf electric field null ($r_0 \approx a$).

If the secondary beam enters the cavity at the same phase as the primary beam, the former will be accelerated if $r_0 > a$, for in this case the rf fields experienced by both beams have opposite polarity [Fig. 2(a)]. Since the rf electric field has a radial dependence of $J_0(\omega r/c)$, it is obvious that $1/|\delta|$ is the "transformer ratio," which is the ratio of the energy gain by the secondary beam to the energy loss by the primary beam, *if both beams enter the cavity at the same phase.* This dependence on the phase is reflected in the following equation which describes the change in the relativistic mass factor (γ_s) of the secondary beam as it traverses the nth cavity:

$$\frac{d\gamma_s}{dn} = -\Lambda\delta\cos(\theta_s - \theta_d)\,, \tag{4}$$

where θ_s is the phase of the secondary beam bunch and θ_d is the phase of the primary beam bunch when they enter the nth cavity. Equation (4) is readily obtained from Eq. (1) by noting the transformer ratio $1/\delta$ and the phase difference mentioned above. Equations (3) and (4) indeed show that γ_s increases if $r_0 > a$ and if $\theta_d = \theta_s$.

The secondary beam cannot be accelerated indefinitely because of the increase in the phase slippage between θ_d and θ_s downstream. This phase slippage occurs as the primary beam is decelerated and the secondary beam is accelerated. Its rate of increase is governed by

$$\frac{d(\theta_s - \theta_d)}{dn} = \frac{\omega L}{c}\left(\frac{1}{\beta_s} - \frac{1}{\beta_d}\right) = \frac{\omega L}{c}[(1 - 1/\gamma_s^2)^{-1/2} - (1 - 1/\gamma_d^2)^{-1/2}]\,. \tag{5}$$

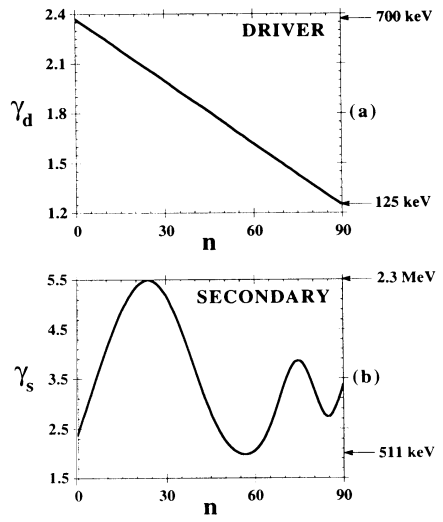

FIG. 3. Evolution of the relativistic mass factors when the driver beam radius r_0 is a constant: (a) the driver beam, (b) the secondary beam. Phase slippage prohibits continual acceleration of the secondary beam.

The effect on the secondary beam by this phase slippage is illustrated in Fig. 3, which is obtained by numerically solving the system of three equations [(1), (4), (5)] in three unknowns: γ_d, γ_s, and $\theta_s - \theta_d$. The initial conditions for these three unknowns are taken to be $\theta_s - \theta_d = 0$ and $\gamma_d = \gamma_s = 2.37$, corresponding to an initial energy of 700 keV for both beams. The other parameters are $\omega/2\pi = 3.65$ GHz, $b = 7.221$ cm, $L = 1$ cm, $a = 3.146$ cm, $r_0 = 3.322$ cm, $Q = 100$, and $I_d = 0.5$ kA. Since we have taken $L = 1$ cm, the cavity number n is also the axial distance (z) in cm.

Figure 3(a) shows that γ_d decreases from the initial value of 2.37 to 1.24 at $n = 90$; i.e., the primary beam's energy steadily decreases from 700 to 125 keV after propagating 90 cm. The secondary beam's energy [Fig. 3(b)] increases initially, reaching a maximum value of 2.3 MeV after 24 cm, and then decreases due to the phase slippage until $n = 56$, and oscillates further downstream as the phase slippage continues.

The phase slippage may be corrected by adjusting the primary beam's radius r_0. Consider, for example, the worst case of phase slippage where the primary beam and the secondary beam arrive at a cavity 180° out of phase, as shown in Fig. 2(b). If the primary beam's radius r_0 is *less* than a, it generates an rf electric field which would retard *both* beams during the time when the *primary* beam occupies the cavity. However, when the charge bunch of the primary beam resides in the cavity, there are few particles in the secondary beam residing in the same cavity because both beams arrive at the cavity 180° out of phase. By the time the charge bunch of the primary beam is about to leave the cavity, the rf electric field is about to change sign, at which time the charge bunch of the secondary beam is about to enter the cavity, whose rf electric field then begins to accelerate the entering bunch

on the secondary beam. Thus, the phase slippage problem can be corrected by a simple cure: At the locations where the bunches of both beams enter the cavity with the same phase, place r_0 outside a. When the bunches of both beams arrive at the cavity 180° out of phase, place r_0 inside a.

Mathematically, it is easy to see from Eqs. (3) and (4) that γ_s is a monotonically increasing function of n if r_0 is tapered in such a way that $(r_0-a)\cos(\theta_s-\theta_d)\geq 0$.

The above idea of phase slippage correction has been tested for the example shown in Figs. 3(a) and 3(b). From that figure, the phase slippage occurs with a period of the order of 75 cm. Thus, we correct the primary beam radius r_0 according to

$$r_0(\text{cm})=3.146+(3.322-3.146)\cos(2\pi n/75). \quad (6)$$

Including only this modification, and keeping all other parameters the same, we obtain Fig. 4. In Fig. 4, we see that the primary beam's energy monotonically decreases from 700 to 400 keV over 90 cm, whereas the secondary beam's energy increases monotonically from 700 keV to a maximum of 4.2 MeV over the same distance, in sharp contrast to Fig. 3(b). The loss of 300 keV in the primary beam and the gain of 3.5 MeV in the secondary beam implies an effective transformer ratio of about (3.5 MeV)/(300 keV)=11.7.

In Fig. 4, the zero slopes in γ_s and in γ_d occur at the axial positions (n) at which the driver beam radius r_0 coincides with the field-null position a. The slight dip in γ_s at $n=90$ only means that the primary beam's radius r_0 needs further adjustment there. If we write $r_0=a+\Delta\cos(\psi)$, where Δ is the amplitude and ψ is the phase of the modulation in r_0, the general phase focusing condition reads $d\psi/dn=d(\theta_s-\theta_d)/dn$. This condition is applicable when the two beams have different velocities. In fact, one might argue that this technique of radius modulation provides both beams with self-focusing in phase, similar to the self-focusing in synchrotrons [15].

The modulation in the annular beam radius may be readily achieved by a proper adjustment of the external solenoidal magnetic field which is often used for beam focusing and beam transport [3–6,14]. Since the rate of change of energy depends on the annular beam radius r_0 [cf. Eqs. (1) and (3)], the output energy of the accelerated beam may also be controlled by the same external magnetic field coils.

The above ideas may be tested in a proof-of-principle experiment with parameters similar to those used to produce Fig. 4. The primary beam may be obtained, for example, from the Michigan Electron Long-Beam Accelerator (MELBA) [16], which operates with diode parameters of 700 keV, current up to 10 kA, and flattop pulse length up to 1 μs. This primary beam may be modulated using the proven techniques by Friedman *et al.* [3,4,6]. Note that the average acceleration gradient of 40 kV/cm and the peak acceleration gradient of about 80 kV/cm implied by Fig. 4 are well within the rf breakdown limit. If we assume an acceleration efficiency of 25%, a secondary beam of more than 10 A of current may be accelerated to 4 MeV in less than a meter in this proof-of-principle experiment.

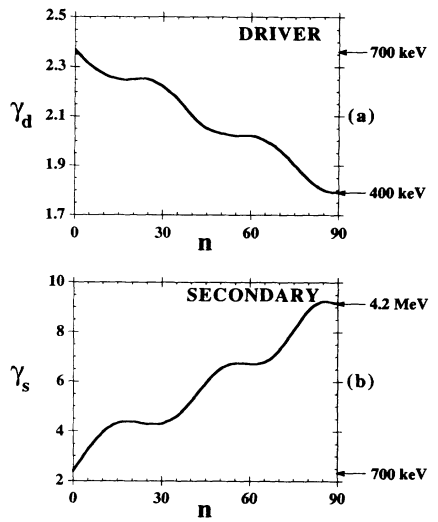

FIG. 4. Evolution of the relativistic mass factors when the driver beam radius r_0 is modulated to compensate phase slippage: (a) the driver beam, (b) the secondary beam.

There are many issues which may affect the eventual usefulness of the two-beam accelerator concept outlined above. Chief among them is the modification of the rf characteristic that always accompanies an intense driver beam, which includes a detuning of the structure frequency and a modification of the gap transit-time factor [4,11,12,17]. Also of concern is the beam breakup instability (BBU) on the driver beam [10,13,14,17]. However, we have recently found that BBU in an annular beam may be far less serious than a pencil beam [18], and BBU can be controlled by many well-known techniques [19]. The degree of coupling among neighboring cavities, especially in the presence of an intense beam, remains to be studied [20]. Although the driver beam's radius is a crucial factor, the effects of the beam's finite thickness are far less important, according to our preliminary studies. We have also examined the effects of the transverse wake [21] and of the longitudinal instabilities [22] and found that they are not serious, at least for the parameters used in the above numerical example, assuming a solenoidal field of 10 kG in the accelerating structure.

In summary, we propose a novel scheme which has the potential of converting many existing pulse power systems into compact rf accelerators that are suitable for industrial and medical applications. The driver beam is a modulated intense relativistic electron beam of annular shape and low energy (<1 MeV). The secondary beam is an on-axis pencil beam. The secondary beam may reach an energy up to 10 MeV in 1 to 2 m. Phase focusing and energy tunability of the accelerated beam may be provided by an external magnetic field, which controls the radius of the primary beam. While we have in this paper con-

centrated only on electron acceleration in the 10 MeV range, it is intriguing to speculate on the potential of using this technique (a) to accelerate ions to tens of MeV, and (b) to accelerate electrons to ultrahigh energy using superconducting cavities [cf. Eq. (2)] and higher energy driver beams.

We thank John W. Luginsland for assistance in the preparation of this manuscript. This work was supported by SDIO-BMD/IST/ONR.

[1] J. C. Martin (unpublished); see also the survey by J. A. Nation, Part. Accel. **10**, 1 (1979).

[2] S. Humphries, *Charged Particle Beams* (Wiley, New York, 1990); R. C. Davidson, *Physics of Nonneutral Plasmas* (Addison-Wesley, Redwood City, CA, 1990); R. B. Miller, *Intense Charged Particle Beams* (Plenum, New York, 1982).

[3] M. Friedman and V. Serlin, Phys. Rev. Lett. **55**, 2860 (1985); M. Friedman *et al.*, J. Appl. Phys. **64**, 3353 (1988); J. Krall and Y. Y. Lau, Appl. Phys. Lett. **52**, 431 (1988).

[4] M. Friedman *et al.*, Rev. Sci. Instrum. **61**, 171 (1990); Y. Y. Lau *et al.*, IEEE Trans. Plasma Sci. **18**, 553 (1990).

[5] See, e.g., Proc. SPIE Int. Soc. Opt. Eng. **1407** (1991); **1629** (1992); **1872** (1993) (edited by H. E. Brandt).

[6] M. Friedman *et al.*, Phys. Rev. Lett. **63**, 2468 (1989).

[7] M. A. Allen *et al.*, Phys. Rev. Lett. **63**, 2472 (1989); A. M. Sessler and S. S. Yu, *ibid.* **58**, 2439 (1987).

[8] G. Voss and T. Weiland, DESY Report No. M82-10, 1982 (unpublished); DESY Report No. M82-079, 1982 (unpublished).

[9] W. Gai *et al.*, Phys. Rev. Lett. **61**, 2765 (1988); H. Figueroa *et al.*, *ibid.* **60**, 2144 (1988); J. B. Rosenzweig *et al.*, Phys. Fluids B **2**, 1376 (1990).

[10] A. M. Sessler *et al.*, Part. Accel. **31**, 1277 (1990); Nucl. Instrum. Methods Phys. Res., Sect. A **306**, 592 (1991); D. B. Hopkins *et al.*, Nucl. Instrum. Methods Phys. Res. **228**, 15 (1984); D. H. Whittum *et al.*, Phys. Rev. A **43**, 294 (1991); also in "Advanced Accelerator Concepts," edited by J. Wurtele, AIP Conf. Proc. No. 279 (AIP, New York, to be published).

[11] P. B. Wilson, in *Physics of High Energy Particle Accelerators*, edited by R. A. Carrigan *et al.*, AIP Conf. Proc. No. 87 (AIP, New York, 1982), p. 452.

[12] D. G. Colombant and Y. Y. Lau, Phys. Rev. Lett. **64**, 2320 (1990).

[13] This is similar to the cumulative beam breakup instability, suggested by W. K. H. Panofsky and M. Bander, Rev. Sci. Instrum. **39**, 206 (1968).

[14] See, e.g., P. R. Menge, R. M. Gilgenbach, and Y. Y. Lau, Phys. Rev. Lett. **69**, 2372 (1992); Y. Y. Lau, *ibid.* **63**, 1141 (1989), and references therein.

[15] See, e.g., E. D. Courant, in *Physics of High Energy Particle Accelerators* (Ref. [11]), p. 2.

[16] R. M. Gilgenbach *et al.*, in *Digest of Fifth IEEE Pulse Power Conference* (IEEE, New York, 1985), p. 126.

[17] P. Menge, Ph.D thesis, University of Michigan, Ann Arbor, 1993.

[18] Y. Y. Lau and J. W. Luginsland, J. Appl. Phys. **74**, 5877 (1993). In the line above Eq. (7) of this paper, the factor $[I/(1\ \mathrm{kA})]$ should read $[I/(17\ \mathrm{kA})]$.

[19] In the absence of other stabilizing mechanisms such as stagger tune and betatron frequency spread, we estimate that a solenoidal magnetic field of 10 kG and a dipole mode Q of 100 would limit the *worst* BBU growth to $1.8e$-fold (in amplitude) for a 500 ns, 0.5 kA beam in a 90 cm accelerator structure, as in the numerical example.

[20] There are several ways to reduce the coupling among neighboring cavities. The inductive coupling at the annular hole, through which the driver beam passes, may be canceled by the capacitive coupling at the center hole, and if necessary, by introducing additional holes near the rf electric field maximum (so as to increase the capacitive coupling) that is close to the outer wall of the cavity (Fig. 1). Alternatively, conducting wires may be inserted radially across the annular gap to reduce the inductive coupling. Multiple pencil beams may also be used as the driver. These pencil beams pass through holes that are distributed annularly. In the event that the neighboring cavities are not completely isolated electromagnetically, a traveling wave formulation would be required; but the radius modulation that is proposed in this paper still provides an external control to ensure phase focusing.

[21] We estimate that a nominal value of solenoidal field $B_0=10$ kG would render the effects of the transverse wake field on the driver beam unimportant. Specifically, under the condition $\Omega \gg \omega/\gamma_d(1+\beta_d)$, where Ω is the nonrelativistic cyclotron frequency associated with B_0 and the other symbols are the same as in Eq. (5), the electron motion is adiabatic along the composite (dc+rf) magnetic field line. The maximum angular displacement, from the mean, is estimated to be $l_\theta=0.52(c/\omega)(E_a/cB_0)\beta_d/(1-\beta_d)$ where E_a is the maximum accelerating electric field experienced by the secondary beam. The maximum radial displacement is $l_r=l_\theta\lambda_L/\lambda_m$, where $\lambda_L=2\pi\beta_d\gamma_d c/\Omega$ and λ_m is the axial wavelength associated with the modulation in the driver beam radius. For the parameters used in the numerical example, $l_\theta \leq 0.2$ cm, and $l_r \leq 0.0058$ cm. The spread in momentum, dp, in the driver beam may introduce a variation in its annular beam radius, dr_0. It is estimated that $dr_0 \leq [2(\lambda_L^2/\lambda_m^2)\Delta+0.083\lambda_L E_a/cB_0]dp/p$, where Δ is the amplitude of the modulation in the driver beam radius. Using the parameters in the numerical example, we find $dr_0<0.0061$ cm if $dp/p<1$. Thus, the effectiveness of radius modulation is not affected by momentum spread.

[22] We conjecture that the longitudinal (Robinson-like) instability probably is not important for the present scheme, at least in the proposed proof-of-principle experiment. Unlike a circular accelerator, the present scheme is single pass. Its acceleration length is quite short; its length is only slightly over one wavelength in the radius modulation. Moreover, the drive frequency may be adjusted to be on the "right side" of the structure frequency to avoid the Robinson-like instability.